JOURNAL OF MATERIALS SCIENCE 30 (1995) 4659–4668

Interactions under hydrostatic pressure of a mild steel with liquid aluminium alloys

Ph. VAILLANT, J. P. PETITET
Laboratoire d'Ingénierie des Matériaux et des Hautes Pressions, CNRS, Institut Galilée, Avenue J.B. Clément, 93430 Villetaneuse, France

Interactions of a mild steel with liquid aluminium alloys have been studied in a pressure range of 0.1 to 350 MPa, and a temperature range from solidus to 750 °C, close to the squeeze casting process conditions. After having carried out the synthesis of previous surveys at atmospheric pressure, the influence of dipping parameters, and especially pressure, along with alloying elements on the intermetallic layer formation and on the mechanical strength of samples have been considered. These results must contribute to the improvement of the processing of steel reinforced aluminium matrix composites by squeeze casting process.

1. Introduction

For automotive applications, properties such as the rigidity, strength, heat resistance, wear resistance and fatigue resistance at high temperature are needed. The use of aluminium matrix composites (AlMC) should be a good means to achieve such properties [1].

In the case of AlMC, reinforcement could be ceramic (Al_2O_3, C, SiC ...) or metallic (e.g. carbon steels, stainless steels) [1–14]. Actually, ceramics are more refractory, rigid and light than metals. Nevertheless, due to their brittleness and weak wetting by liquid aluminium, AlMC reinforced with ceramic are difficult to process [15] and present a typical decrease of toughness [13, 14]. The use of ductile reinforcement such as carbon steels or stainless steels limits this disadvantage, improves mechanical properties and decreases costs [1, 4, 13, 14]. AlMC mechanicals properties depend on the matrix, the reinforcement and the interface. Without reaction, the physical and mechanical natures of the bond between matrix and reinforcement determine the mechanical properties of composite [16]. If reactions take place, properties (thickness, morphology) depend on the compounds formed and the adhesion at interfaces [16].

Liquid aluminium strongly reacts with iron and forms brittle intermetallic compounds at the reinforcement–matrix interface (Fig. 1) [17–36] part of which is dissolved in the matrix. To warrant mechanical strength of ferrous alloy reinforced AlMC, it is necessary to form a continuous metallurgical bond between matrix and reinforcement, and to limit the thickness and the dissolution of the intermetallic layer.

The squeeze casting (SC) process [37] is a suitable process for AlMC processing [1, 2, 4, 10, 11, 13, 14]. A known amount of liquid alloy is cast in a metallic die and squeezed until complete solidification of the alloy. The casting temperature depends on the liquidus and the solidification interval of the alloy. In the case of aluminium alloys, casting temperature is fixed between 10° and 100° above the liquidus. The casting pressure depends on the alloy and on the drawing of the piece. In the case of an alloy with a wide interval of solidification, the pressure is around 30 MPa, whereas for an alloy with a short interval of solidification, the pressure is around 100 MPa. During the process, the pressure forces the metal to pour into the die. It avoids porosity, and improves the contact metal – die coating – die, increasing the solidification rate. Therefore pieces manufactured by SC process have no defects due to shrinkage cavities and/or gas porosity and have a fine microstructure. In the case of AlMC processing, the reinforcement (preform or insert) is set into the die before the casting. Process parameters (casting pressure, casting temperature, reinforcement temperature, die and piston temperature) are adjusted [38, 39]. The contact time between the reinforcement and the matrix up to complete solidification is around 18 s [7]. On the other hand, transformation temperatures of compounds depend on pressure [40–45]. With a few exceptions such as silicon, germanium, and bismuth, melting temperatures increase with the pressure increase. These variations have consequences on phase equilibria. For instance, Petitet [45] showed that the increase of the pressure (from 0.1 to 400 MPa) shifts the eutectic point, and the solid solubility of silicon in aluminium of a modified eutectic aluminium–silicon alloy (AS12UN) towards more rich silicon concentrations.

Eutectic

$$T_e = 569 + 3.5 \times 10^{-2} P \quad (1)$$

$$C_e = 12 + 3.7 \times 10^{-3} P \quad (2)$$

where T_e(°C) is the eutectic temperature, C_e (wt %) is the eutectic concentration, and P is the pressure (MPa).

Solid solubility of silicon in aluminium

$$C_s^{Si/Al} = 1.9 + 7.45 \times 10^{-3} P \quad (3)$$

where $C_s^{Si/Al}$ (wt %) is the solid solubility of silicon in aluminium. This shift may explain the improvement

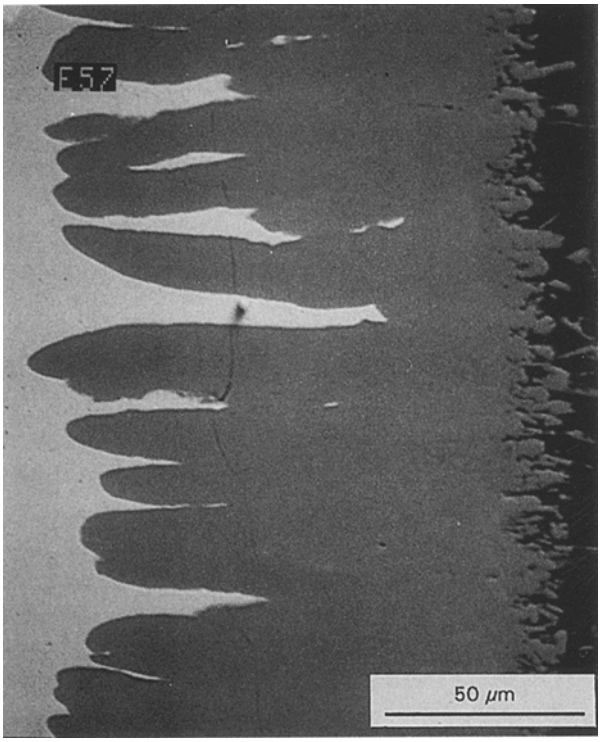

Figure 1 Intermetallic layers after dipping a mild steel in a commercial aluminium–copper alloy. 700 °C, 150 MPa, 600 s.

of the ductility without any loss of strength of aluminium–silicon alloys manufactured by the SC process [41]. Petitet also noticed that the liquidus temperature changes as a function of the pressure

$$T_l = 575 - 5.7 \times 10^{-2} P \quad (P < 50\,\text{MPa}) \quad (4)$$

$$T_l = 568 + 5.8 \times 10^{-2} P \quad (P > 50\,\text{MPa}) \quad (5)$$

where T_l(°C) is the liquidus of the alloy.

After a review of recent works on Al–Fe interactions, new results about the interaction of a mild steel with liquid aluminium alloys in conditions of SC process will be described.

2. Interactions of iron with liquid aluminium

2.1. Fe–Al intermetallic compounds

Intermetallic compounds have a well defined crystal structure, but exist within an extended composition range [46]. The iron–aluminium equilibrium diagram developed by Hansen [48], indicates three stable intermetallic compounds ($\zeta FeAl_2$, ηFe_2Al_5 and $\theta FeAl_3$) in conditions close to the SC process temperatures (solidus 800 °C). At 49 wt % aluminium, the $\zeta FeAl_2$ compound appears. Bradley [49] suggested that the structure was probably monoclinic. The intermetallic compound ηFe_2Al_5, is produced by a congruent melting reaction at 1173 °C and 55 wt % aluminium [19]. Heumann [27] and Schubert [50] showed that this compound is orthorhombic with the c axis statistically occupied with aluminium atoms; remaining sites being vacant. Boundaries of the ηFe_2Al_5 compound given as a compromise by Hansen [48] range from 53 to 56 wt % aluminium. At 1159 °C, a peritectic reaction between the melt and ηFe_2Al_5 produces $\theta FeAl_3$. The composition ranges from 56 to 57.5 wt % aluminium and the structure is monoclinic. Recently Griger [51, 52] confirmed the structure of these compounds, but showed that the peritectic reaction suggested by Hansen was in fact an eutectic reaction (1148 ± 1 °C and 57.3 ± 0.5 wt % aluminium). The $\theta FeAl_3$ composition ranges from 57.8 ± 0.3 to 61.4 ± 0.2 wt % aluminium, whereas between 56.0 ± 0.2 and 57.8 ± 0.3, ηFe_2Al_5 and $\theta FeAl_3$ coexist. Apart from the above three intermetallic compounds, at least two other are reported in this range of temperature. Fe_2Al_7 is reported to exist and to be stable, although no crystallographic evidence has been confirmed [29], However, $FeAl_6$ has been recognized as metastable and has an orthorhombic structure [53].

2.2. The growth of Intermetallics during reactions of solid iron with liquid aluminium

Liquid aluminium perfectly wets iron without oxidation [54]. Two phenomena simultaneously take place at the interface: the dissolution of iron into liquid aluminium and the formation and growth of an alloy layer made of intermetallic compounds by the migration of molten aluminium into iron [1]. The layer is mainly made of ηFe_2Al_5 adjacent to iron $\theta FeAl_3$ adjacent to liquid aluminium [18–37]. It is known, that the growth direction of ηFe_2Al_5 coincides with the direction of the c axis of orthorhombic cells explaining the rapid growth of the layer and the tongue-like shape of the ηFe_2Al_5–iron interface [27] (Fig. 1). In some cases, porosity is observed in ηFe_2Al_5 [19, 55]. The growth rate of the intermetallic layer depends on the growth rate of the two compounds and on the dissolution rate of $\theta FeAl_3$.

2.2.1. The dissolution does not take place in the case of iron saturated molten aluminium

The intermetallic layer growth rate is limited by the diffusion of reacting species through the intermetallic layer and not by interface chemical reactions [1, 36, 56]. Consequently, the rate is inversely proportional to the interlayer thickness x(m)

$$\frac{dx}{dt} = \frac{k_p}{x} \quad (6)$$

where k_p is the parabolic growth rate constant ($m^2 s^{-1}$) and t(s) the contact time. The intermetallic layer thickness increases in accordance with the parabolic law (initial conditions: $x = 0$ at $t = 0$

$$x = (2k_p t)^{\frac{1}{2}} \quad (7)$$

k_p obeys a simple Arrhenius-type relationship. Dybkov [57, 58] established a more complex model taking into account not only rates of the diffusional transport of reacting species through growing layers but also rates of chemical reactions taking place at interfaces. Heumann [27], by measuring the specific maximum

diffusion distance using pure iron and iron saturated aluminium for times up to 16 min at 715°, 846° and 944 °C, was able to show a linear relationship between the thickness of the intermetallic layer produced, and the square root of the time ($k_p \approx 1 \times 10^{-10}\,m^2\,s^{-1}$ at 715 °C). An Arrhenius plot of this data was linear and yielded an activation energy of 54.8 kJ mol^{-1} attributed to the interdiffusion coefficient of ηFe_2Al_5.

2.2.2. Dissolution takes place in the case of pure liquid aluminium

Because liquid aluminium is always saturated by iron at the $\theta FeAl_3$–molten aluminium interface [36], the dissolution of $\theta FeAl_3$ is limited by the iron transport (the diffusion and/or the convection) in molten aluminium [59]. Yeremenko pointed out the effect of the dissolution on the intermetallic layer growth [34, 35]. Experimental studies were performed by the rotating disc technique. Using the parabolic law for one intermetallic layer growth and the Nernst theory for the dissolution of metals in liquid metals, an equation describing the diffusion controlled growth of the intermetallic layer in case of pure aluminium has been derived

$$\frac{dx}{dt} = \frac{k_p}{x} - \frac{C_s^{Fe/Al} K}{\rho_{int}\phi} \exp\left(-\frac{KS}{V}t\right) \qquad (8)$$

where $C_s^{Fe/Al}$(kg m^{-3}) is the saturation concentration of iron in molten aluminium, K (m^2 s^{-1}) is the dissolution rate constant, S(m^2) is the specimen surface area, V(m^3) is the melt volume, ρ_{int}(kg m^{-3}) is the specific mass of ηFe_2Al_5 and ϕ is the mass fraction of iron in ηFe_2Al_5. The following data were used for calculations at 700 °C: $C_s^{Fe/Al} = 60 \pm 3\,kg\,m^{-3}$; $K = (3.8 \pm 0.1) \times 10^{-5}\,m^2\,s^{-1}$; $\rho_{int} = (4.1 \pm 0.1) \times 10^3\,kg\,m^{-3}$; and $\phi = 0.453$. The thickness–time relationship was in accordance with experimental data. However, Eggeler [22] proved that the iron enrichment occurs not only with the dissolution, but also by separating little particles of intermetallic layer.

2.3. The effects of alloying additions on the intermetallic layer

The intermetallic layer formed between ferrous alloys (carbon steel, low alloyed steel, cast iron) and pure molten aluminium is mainly composed of ηFe_2Al_5 near the insert and $\theta FeAl_3$ near aluminium, and has a tongue-like ηFe_2Al_5–insert interface [18–20, 22, 28, 32]. Interesting results were obtained by Uchida [33] who dipped a low carbon steel into iron-saturated aluminium alloy 3.2 wt % of iron) for times ranging from 1 to 30 s at 730 °C. The intermetallic layer is composed of the two well known compounds. The increase of the intermetallic layer thickness with the dipping time is divided into two parabolic growth steps. He considered that the growth of the intermetallic layer was controlled by an internal diffusion of aluminium through $\theta FeAl_3$ in the first step (times < 10 s) and through ηFe_2Al_5 in the second step (times > 10 s). Niinomi [32] dipped commercially pure iron, iron–silicon, iron–chromium, iron–nickel, iron–manganese, iron–copper and iron–carbon alloys (2–3 wt % of alloying elements) into molten aluminium at 700°, 750° and 800 °C for various times. Alloying additions, and specially silicon, nickel, and copper, reduce the intermetallic layer thickness. In the case of carbon, the ferrous alloy–aluminium interface is not tongue-like. Silicon, chromium, nickel, manganese and copper are present in the intermetallic layer and silicon was enriched at the ferrous alloy–intermetallic interface and at the intermetallic–aluminium interface. He suggested that a ternary Fe–Al–Si compound might be formed in the Si-rich region but the existence of the compound is not confirmed. Komatsu [28] showed that a high silicon layer was formed when the silicon content in Fe–Si alloys was higher than a certain limit (about 3 wt % of Si). He determined the solubility limit of silicon in a columnar layer to be $\approx$ 2–3 wt % of silicon. The absence of carbon in the intermetallic layer could be readily understood because carbon cannot diffuse through iron–aluminium intermetallics, presumably due to a low solubility in such compounds [19]. Colin [54] showed that lamellar graphite in grey cast iron had a more efficient effect on the intermetallic layer thickness than cementite in low carbon steel, because lamellar graphite forms a tridimensional array and acts as a diffusional barrier.

The influence of alloying additions in aluminium on interactions of ferrous alloys with liquid aluminium alloys has been described [19]. Silicon is the most important element of addition. It is known that silicon as an addition to molten aluminium strongly reduces the intermetallic layer thickness [23, 26, 28, 30, 31, 34, 37]. Nicholls [31] assumed, that silicon atoms occupied structural vacancies of ηFe_2Al_5 which has good diffusion facilities [27, 50]. Eggeler [23] confirmed these results in reactions between a low alloyed steel and pure aluminium melt and a 2 wt % silicon-containing aluminium melt at 780° and 792 °C. The velocity of the iron enrichment is the same for both cases, whereas the intermetallic layer growth is much faster with pure aluminium melt. Silicon is found to be incorporated in the intermetallic layer. From these results, Eggeler [23] claimed that silicon acts on the solid state side. Other authors take the view that intermetallic compounds Al–Fe–Si are formed, growing more slowly than ηFe_2Al_5. Uchida [33] reported that in 2.5 wt % silicon-containing aluminium the intermetallic layer was composed of ηFe_2Al_5, $\theta FeAl_3$ and αAlFeSi; whereas in an 8 wt % silicon containing aluminium, the intermetallic layer is composed only of the outermost intermetallic compound αAlFeSi. He observed that the wetting force between steel sheets and pure molten aluminium was as high as 400 mJ m^{-2}, but that between steel sheets and molten aluminium containing 8 wt % of silicon in which the growth of the intermetallic layer was not always detected, was about 50 mJ m^{-2}. He considered that αAlFeSi has inhibition effects on the reaction between steel sheets and molten aluminium–silicon alloys. However, Komatsu [28] made weight loss studies with different aluminium–silicon alloys and reported that silicon does not inhibit the intermetallic layer growth, but accelerated

TABLE I Chemical composition of AS10G and AU5GT used as the matrix in this study

Material	Element wt %	Si	Fe	Cu	Mn	Mg	Ni	Zn	Pb + Sn	Na	Ti	Others
AS10G	minimum	9.000				0.300				0.003	0.080	
	maximum	10.0	0.14	0.20	0.040	0.400	0.020	0.040	0.020	0.012	0.130	0.100
	(±)	0.300	0.010	0.010	0.010	0.020	0.010	0.010	0.010	0.001	0.010	
AU5GT	minimum		0.120	4.3		0.250					0.170	
	maximum	0.130	0.230	4.9	0.090	0.350	0.040	0.090	0.020		0.230	
	(±)	0.400	0.020	0.1	0.010	0.020	0.010	0.010	0.010		0.020	

its dissolution into liquid aluminium. Jones [36] argued that silicon accelerates the iron solubility into aluminium, as follows from the Al–Fe–Si system reported by Rivlin [60].

2.4. Mechanical aspects of the interface

In the case of ferrous alloy reinforced AlMC, interfacial reactions between the reinforcement and the matrix often take place during the elaboration [1, 2–5, 12, 13, 16, 26, 61–63]. Best results are observed when a continuous intermetallic layer is formed at the reinforcement–matrix interface [26]. It is known that Fe–Al intermetallic compounds are brittle. According to Nishida [44], H_v microhardness of ηFe_2Al_5 ranges from 870 to 1020, ($\eta Fe_2Al_5 + \theta FeAl_3$) from 670 to 870 and $\theta FeAl_3$ from 670 to 780. Due to their brittleness, the formed intermetallic layer fractures at small strain. Chemical reactions at interfaces tend to degrade basic properties of the reinforcement and to increase residual stresses at composite interfaces [16]. For these reasons, it appears necessary to limit the thickness of the intermetallic layer. Nevertheless, there is no theoretical model joining the longitudinal strength of these composites to a critical thickness of the brittle layer as with brittle fibre–reinforced metal matrix composites [62]. Gürtler [26] reported that the tensile and the shear strength of test pieces manufactured by the Al-Fin process were improved by reducing the intermetallic layer and ranged respectively from 59 to 119 MPa and from 39 to 59 MPa. Dybkov [20] showed, that mechanical tensile properties of aluminium alloys/stainless steel pipes and these of the starting melt materials appeared to be the same. The rupture of bimetallic pieces always appeared in the aluminium part. Direct measurement of the interface strength is obtained by the pullout test. Kelly [17] extensively used the pullout test to determine the stress transfer from the matrix to the fibre around the fibre ends. Using a simple shear lag analysis, he determined the shear strength of the interface (for a perfectly plastic matrix) as

$$\tau_i = \frac{\sigma_f d}{2l_c} \quad (9)$$

where l_c(m) is the critical length of the fibre, d(m) is the diameter of the fibre, τ_i(MPa) is the shear strength of the interface and σ_f(MPa) the stress exerted on the fibre. By embedding various lengths of the fibre (l) into the matrix, the quantity l/d can be varied, and l_c established as the length at which the failure mode changes from pullout fibre fracture. This was criticized by Metcalfe [16], mainly because the stress distribution within the specimen is more complex than that assumed by the shear lag analysis.

Except for a few papers [1–5, 13, 14, 63], the major part of the work on interactions of ferrous alloys with liquid aluminium alloys has been performed at atmospheric pressure. If the SC process is known to improve mechanical properties of parts of aluminium alloys [38], possibilities and conditions for manufacturing ferrous alloy reinforced AlMC are less well known. The objective of this present work is to study the influence of pressure on the nature, the kinetic and the mechanical strength of intermetallic interfaces by a series of experimental observations.

3. Experimental methods

A classical mild steel (XC18) was used as an insert (0.16–0.22 wt % C, 0.40–0.70 wt % Mn, 0.15–0.35 wt % Si, 0.40 wt % Cr, 0.40 wt % Ni, 0.10 wt % Mo and 0.035 wt % P). Inserts had a diameter of 2 mm and a straightened length of 17 mm. The composition of the two commercial aluminium alloys used as a matrix, AS10G and AU5GT, are shown in Table I. The first is a casting alloy and has a short interval of solidification (560–590 °C), whereas the second is a forging alloy and has a wide interval of solidification (540–650 °C). Matrix samples were cylindrical (8 × 8 mm). On the other hand, pure iron (99.9985 wt %) and pure aluminium (99 wt %) samples were also used as an experimental reference. For the study of aluminium–silicon alloys, 2, 4, 5, 6, 8 and 10 wt % silicon were alloyed to the aluminium. Samples were normalized, ground, polished and cleaned before dipping.

Dipping tests were carried out in a high pressure vessel (0.1–350 MPa) containing a furnace (20–800 °C) as shown in Fig. 2. A dipping device enables two materials to be brought into contact. A thermocouple (K) is placed inside the insert and enables the temperature next to the contact zone to be detected. Dipping conditions are presented in Table II. Differential thermic analysis measurements were performed to determine the variation of liquidus temperatures (590 °C for AS10G and 650 °C for AU5GT) as a function of the pressure. The liquidus temperature of AS10G and AU5GT increases as a function of the pressure

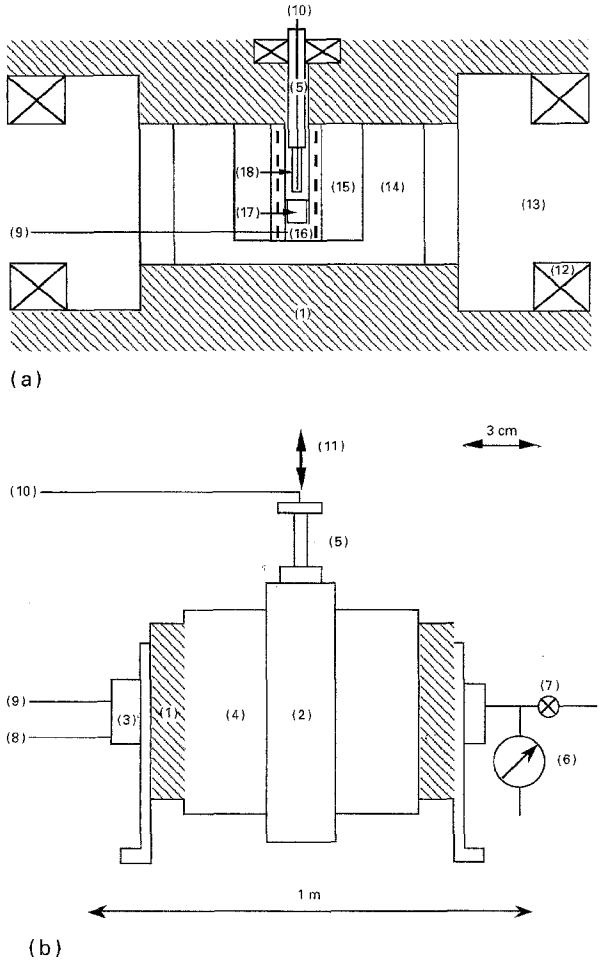

Figure 2 (a) Schematic diagram of the high pressure dipping device used in this work. (b) One part of the cross-section of the high pressure dipping device. (1) high pressure vessel, (2) binder, (3) breech, (4) water cooling, (5) dipping device, (6) high pressure resistive gauge, (7) valve, (8) feed through, (9) thermocouple of regulation, (10) thermocouple of measurement, (11) hydraulic double effect jack, (12) joint, (13) plug, (14) buffer, (15) furnace, (16) crucible, (17) matrix, (18) insert.

(0.1–350 MPa) according to a linear relationship

$$\text{AS10G: } T_l = 589 + 6.2 \times 10^{-2} P \quad (10)$$

$$\text{AU5GT: } T_l = 648 + 7.4 \times 10^{-2} P \quad (11)$$

where T_l is the liquidus temperature (°C), and P(MPa) the pressure. Matrix samples were set into a boron nitride crucible and insert samples screwed on the dipping device. Inserts were dipped under pressure (argon) at a constant rate (5 mm s^{-1}) and a constant depth (7 mm) into the melt. The bath temperature was monitored by a K thermocouple (± 5 °C). The dipping pressure was measured by a high pressure resistive gauge (± 1 MPa). Samples were solidified under pressure (5° s^{-1}). Some of them were submitted to a solution heat-treatment (AS10G: 525 °C for 12 h, mild water quenched at 160 °C for 6 h; AU5GT: 540 °C for 10 h, mild water quenched at 180 °C for 12 h). Bimetallic samples obtained were cut at right angles to the insert, and polished up to 1 μm. They were observed by scanning electron microscopy (SEM, backscattered electrons). The intermetallic layer thicknesses were measured by image processing. Analysis of the chemical compositions of intermetallics were performed near the centre of each one with

TABLE II Dipping conditions

Insert	mild steel (XC18)		
Matrix	AS10G		AU5GT
Pressure (MPa)		0.1, 50, 150, 300	
Temperature (°C)	600, 700		570, 650, 750
Time (s)		18, 120, 600	

TABLE III Composition measured by EDA(wt %) of the two layers between pure aluminium/iron or mild steel. Dipping conditions: 700 °C, 150 MPa, 600 sec

	Layer I (near insert)		Layer II (near matrix)	
Specimens	Al	Fe	Al	Fe
Aluminium–Iron	55	45	61	39
Aluminium–mild steel	57	43	61	39

Pure iron–pure liquid aluminium, mild steel–pure liquid aluminium and mild steel–liquid aluminium silicon alloys were dipped under 150 MPa during 18, 120 and 600 s at 700 °C.

a SEM using energy dispersive analysis (EDA). Concentration profiles and concentration measurements in the reaction zone were recorded using a CAMECA-Camebax KMX microanalyser. Vickers microhardness measurements were made. Pullout tests were carried out on an Instron device with a traction rate of 0.02 cm min^{-1} and a stress ranging from 0 to 981 N. Bimetallic samples were normalized and the bottom polished to observe pullout insert.

4. Results and discussion

4.1. The effects of alloying elements on intermetallics under pressure

After dipping pure iron into pure aluminium melt under pressure, at conditions mentioned above, the intermetallic layer consists of two compounds which are the same than those obtained at atmospheric pressure: ηFe_2Al_5 (layer I) near to the iron insert, and $\theta FeAl_3$.(layer II) near to the matrix (Table III). Only the thickness of the ηFe_2Al_5 compound increases with time which is in accordance with Uchida's assumptions [33]. Intermetallic needles are observed in the matrix and its composition is close to θFe_2Al_3. They are due to the precipitation of dissolved iron into the matrix, but also by the separation of little particles of the $\theta FeAl_3$. Their morphology depends on the cooling rate [22]. Because of these phenomena, the parabolic time relationship is not observed. In all cases, aluminium is not detected in the insert (iron or mild steel). All the diffusing aluminium may be consumed at the insert–intermetallic layer interface by the formation of ηFe_2Al_5. The use of a mild steel as an insert does not affect the formation of intermetallics, but decreases the thickness of the layer as one can observe in Fig. 3.

The use of AU5GT as matrix above the liquidus does not affect sensitively the nature of intermetallic compounds (Table IV, Fig. 4a), but decreases the intermetallic layer thickness (Fig. 3). Copper is present, at less than 1 wt % in the chemical composition of the

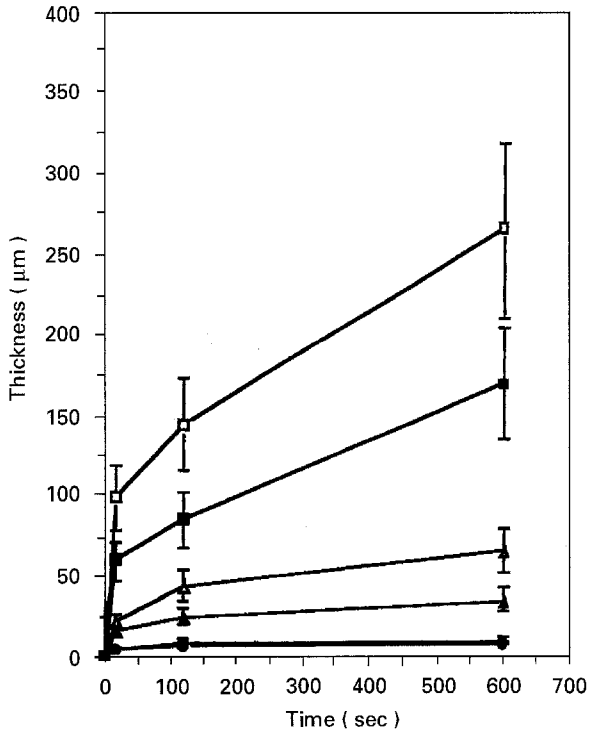

Figure 3 Relation between thickness of the intermetallic layer and dipping time independent of pressure. □ Al–Fe 700 °C; ■ Al–mild steel 700 °C; △ AU5GT–mild steel 700 °C; ▲ AU5GT–mild steel 650 °C; ○ AS10G–mild steel 700 °C; ● AS10G–mild steel 600 °C.

TABLE IV Composition measured by EDA (wt %) of the two layers between AU5GT and a mild steel

	Layer I (near insert)			Layer II (near matrix)		
AU5GT/Mild steel	Al	Fe	Cu	Al	Fe	Cu
750 °C, 150 MPa, 600 s	58.9	43.3	<1	63.6	38.6	<1
750 °C, 150 MPa, 18 s, heat treated	56	44	0	48	13	38
570 °C, 150 MPa, 600 s	55	45	0	55	14	31

two compounds, and may explain the decrease of the measured intermetallic layer thickness. When experiments are carried out at atmospheric pressure, porosity is present in ηFe_2Al_5 as one can observe in Fig. 4b. If the temperature is below the liquidus (Fig. 5), the intermetallic adjacent to the insert (layer I) does not show the typical tongue-like interface and its composition is close to ηFe_2Al_5 and $\theta FeAl_3$. On the other hand, the intermetallic adjacent to AU5GT (layer II) shows a rich concentration in copper (Table V). Its composition is close to βCu_2FeAl_7 [65, 66]. These experiments have only been performed at 600 s. Nevertheless, a heat treatment carried on bimetallic samples dipped above the liquidus during 18 s (Fig. 6a) generates the formation of, probably a βCu_2FeAl_7 compound (layer II) (Fig. 6b) by the diffusion of copper during the solution heat treatment from the matrix into $\theta FeAl_3$.

In the case of AS10G, the formation of ηFe_2Al_5 is never observed. For short times, little pits of intermetallics are present at surface of the mild steel, and

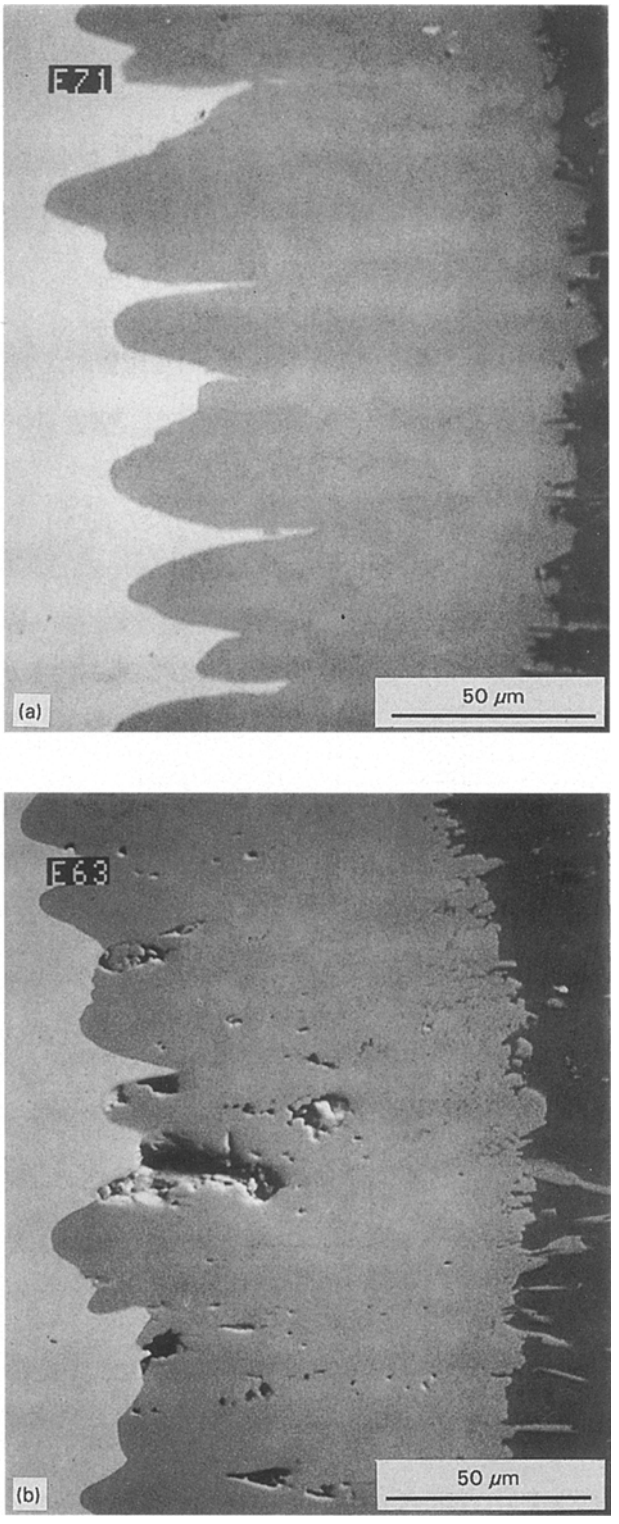

Figure 4 Intermetallic layers after dipping XC18 insert in AU5GT alloy, 750 °C, 600 s. (a) 300 MPa; (b) 0.1 MPa.

quantitative analysis is not available. Nevertheless, silicon is present in the composition of the intermetallic layer. These pits grow with time to form a continuous layer. Microanalysis measurements have been carried out on samples dipped for 600 s. Compositions measured are in accordance with the ternary Al–Fe–Si system as developed by Stefaniay [67]. Under pressure (Fig. 7a), the intermetallic layer is formed by two intermetallic compounds: θAlFeSi adjacent to the insert (layer I) and αAlFeSi adjacent (layer II) to AS10G. At atmospheric pressure (Fig. 7b), the inter-

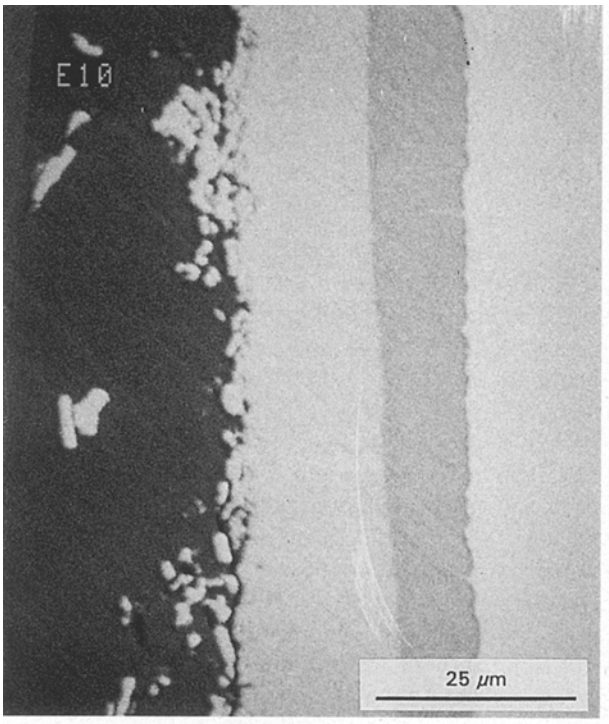

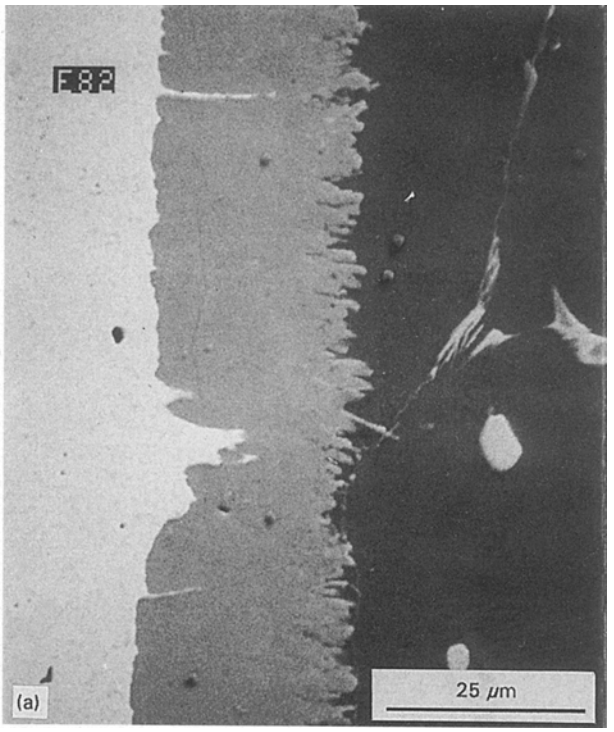

Figure 5 Intermetallic layers after dipping XC18 insert in AU5GT alloy, 570 °C, 600 s, 50 MPa.

TABLE V Composition (wt %) measured by microanalysis measurements of intermetallic layers between a commercial aluminium–silicon alloy and a mild steel

	Atmospheric pressure			Under pressure (300 MPa)		
AS10G/XC18	Al	Fe	Si	Al	Fe	Si
Layer I	55.1	44.1	3.8	52.2	44.6	4.8
Layer II	58.6	33.1	11.7	55.9	33.4	12.2
Layer III	59.2	27.1	17.4			

metallic layer is formed by three intermetallic compounds: θAlFeSi adjacent to the insert (layer I), then αAlFeSi (layer II), and then βAlFeSi adjacent to AS10G (layer III). In both cases, silicon-rich precipitates are detected in θAlFeSi [28, 55] and the formation of aluminium–silicon eutectic is observed around the intermetallic layer. There is some indication [69] that primary silicon or eutectic in aluminium–silicon eutectic alloys nucleate preferentially on the surfaces of reinforcements (carbon, alumina and silicon carbide). Similar observations have been made where magnesium or zinc are the primary phases [13, 69]. In particular, the formation of aluminium–zinc eutectic around reinforcements has been observed in the case of elaboration of continuous steel fibres reinforced with AlMC by the SC process and generates a natural protection of fibres [13]. Results are compared with those obtained with aluminium–silicon alloys.

4.1.1. Alloys containing less than 4 wt % in silicon

The intermetallic layer is formed by two compounds, and compositions of the intermetallic layer correspond to compositions of $\eta Fe_2Al_5(Si)$ and $\theta FeAl_3(Si)$

Figure 6 Intermetallic layers after dipping XC18 insert in AU5GT alloy, 750 °C, 18 s, 50 MPa. (a) not heat treated; (b) heat treated.

from the ternary Al–Fe–Si system developed by Stefaniay [67]. The silicon concentration measured by EDA is about 3 wt % in both compounds. Experimental results confirm the assumption of Nicholls [31] and Eggeler [22], who supposed that silicon changes diffusion conditions into ηFe_2Al_5. For those silicon concentrations, changes in the iron solubility [60] and in the viscosity [68] are negligible. The presence of silicon only results in a slower solid state growth.

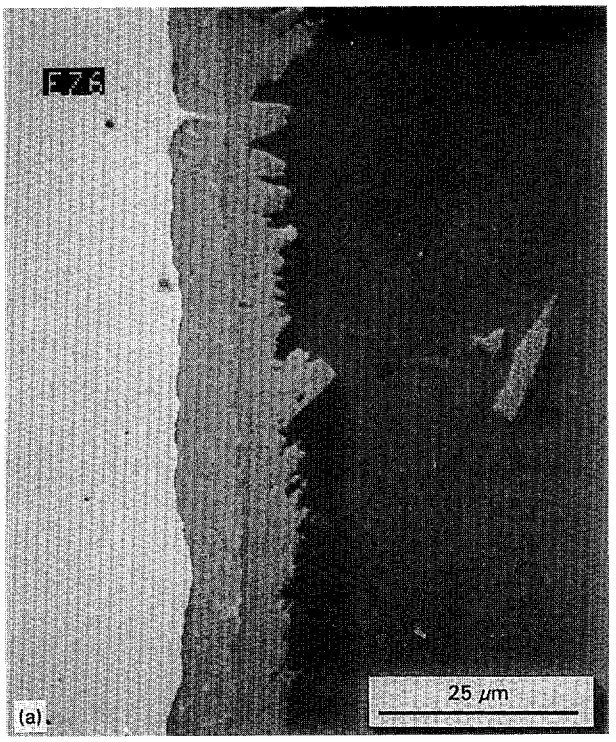

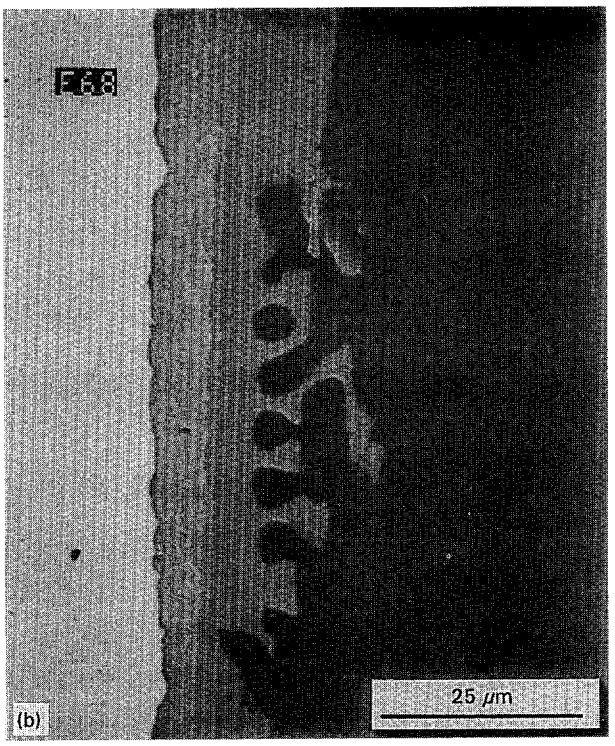

Figure 7 Intermetallic layers after dipping XC18 insert in AU5GT alloy. 700 °C, 600 s. (a) 300 MPa; (b) 0.1 MPa.

4.1.2. Alloys containing more than 4 wt % in silicon

The composition of the two intermetallic compounds are close to those observed at the same conditions with AS10G. The increase of silicon concentration into the alloy reduces the thickness of the layer. Two reasons could explain this phenomenon: first, formed ternary intermetallic compounds grow more slowly than ηFe_2Al_5 [23, 30]; second, silicon accelerates the iron dissolution by increasing the iron solubility into the melt (≈ 2 wt % in pure aluminium and ≈ 7.5 wt % in an aluminium–silicon alloy containing 10 wt % of silicon at 700 °C) [28, 37, 60]. Nevertheless, our results and previous work show that silicon inhibits reactions of ferrous alloys with liquid aluminium–silicon alloys which could be explained by the formation of αAlFeSi [34] and by the increase of the activation coefficient of aluminium into iron [70].

4.2. The influence of pressure

It is known that pressure decreases the diffusion process in solids if the activation volume is positive or equal to zero [56]. Nevertheless, this behaviour is weak [71–74] and depends on solid morphology (mono- or polycrystalline, microstructure) [71]. Our experimental conditions do not allow us to detect the evolution of the diffusion process through the intermetallic layer. On the other hand, the dissolution phenomenon complicates the exact knowledge of the intermetallic layer growth. In accordance with our observations, the application of a pressure up to 300 MPa does not significantly affect the intermetallic layer growth.

Transformation temperatures of compounds depend on pressure. These variations have consequences on phase equilibria as shown in the liquidus temperatures [45] and the interaction of a mild steel with liquid AS10G. This system is different because the melting point of silicon decreases as a function of the increasing pressure [40–45]. Phase equilibria of the Al–Fe–Si system [67] are shifted by increasing the pressure towards rich silicon concentration. Consequently, the outermost layer is less rich in silicon and βAlFeSi does not appear. This assumption is confirmed by the important peak of silicon observed in the matrix at the intermetallic layer–AS10G interface (Fig. 8a and b).

Furthermore, the pressure has mechanical effects on the mechanical strength of samples. First, the pressure increases mechanical properties of matrix [39, 41]. Particularly, the shrinkage around the insert is suppressed by a frettaging effect. Second, a pressure of 50 MPa allows us to avoid porosity into ηFe_2Al_5 (Fig. 5a and b) probably because the dipping temperature is above the brittle–ductile temperature transition (= 2/3 of the melting point of the intermetallic i.e. 550 °C) of ηFe_2Al_5 [64].

4.3. Mechanical strength of samples

Microhardness measurements of ηFe_2Al_5, 960 ± 60 H_v, are in accordance with previous works [44] and confirm the brittleness of this compound. Measurements on other intermetallics are not available because their thickness is too low.

Pullout tests have been performed on representative samples (Table VI). The formation, even located, of an intermetallic layer between matrix and insert increases the pullout strength. Indeed, the worst results are obtained with oxidized inserts before dipping.

4.3.1. AU5GT matrix

The intermetallic layer is continuous and less thick than in the case of aluminium matrix. For samples

TABLE VI Pullout tests

	Oxidized insert		Non-oxidized insert	
Pressure (MPa)	0.1	50	0.1	50
AS10G-XC18;	Pull out	Pullout	Pullout	Pullout
700 °C, 18 s	(≈550 N)	(≈550 N)	(≈800 N)	(≈800 N)
AU5GT-XC18;	Pull out	Pullout	Pullout	Fracture
750 °C, 18 s	(≈550N)	(≈550 N)	(≈800 N)	(≈980 N)

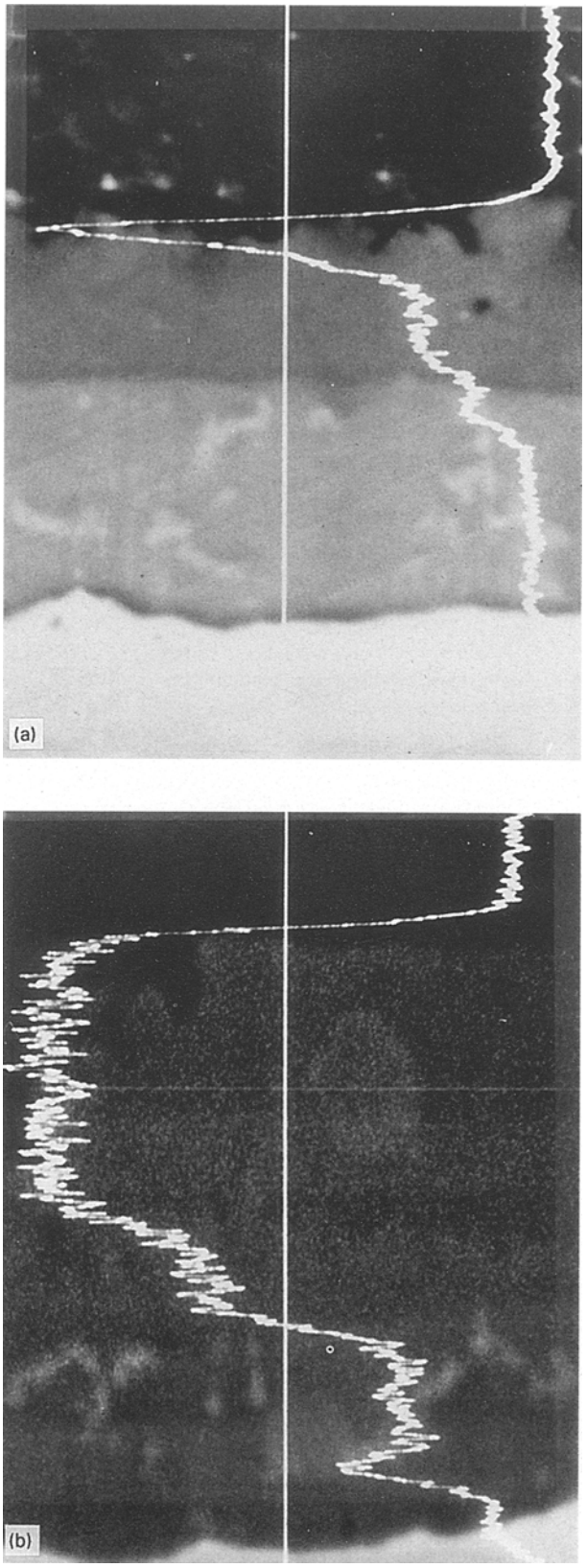

Figure 8 Concentration profile of silicon in the intermetallic layers, 700 °C, 600 s. (a) 300 MPa; (b) 0.1 MPa.

dipped at atmospheric pressure, the pullout of the insert is due to the shrinkage of the matrix around the intermetallic layer. Insert fractures are observed in the case of samples dipped under pressure because there is no shrinkage around the intermetallic layer.

4.3.2. AS10G matrix

A great decrease of the intermetallic layer thickness is observed. Nevertheless, the layer is not continuous and causes insert pullout because of insert–matrix debonding.

5. Conclusions

This work simultaneously analyses the effect of the manufacturing parameters and alloying additions on the morphology, the nature and the formation of the intermetallic layer between iron and liquid aluminium in the SC process conditions. Results show that aluminium alloying additions have a great influence on the interactions of a mild steel with liquid aluminium alloys. In the case of copper, the nature of intermetallic compounds depends on the dipping temperature and on the heat treatment, whereas in the case of silicon, it depends on the silicon concentration in the aluminium alloy and on the dipping pressure. We have determined the SC process conditions involving the formation of a continuous intermetallic layer between a mild steel and a commercial aluminium–copper alloy, allowing a good pullout strength to our specimens. It is not the case with a commercial aluminium–silicon alloy because silicon inhibits reactions between ferrous alloys and liquid aluminium alloys.

Acknowledgements

The authors wish to thank Renault Automobiles Co. for financial support.

References

1. F. BARBIER and M. H. AMBROISE, in Proceedings of the Eighth International Conference on Composite Materials, Honolulu, July 15–19, 1991, edited by W. Tsai and G. S. Springer (Society for the Advancement of Material and Process, 1991) 18, p. J1.
2. R. B. BHAGAT, in Proceedings of the First European Conference on Composite Materials, Bordeaux, France (September 1985) p. 610.
3. R. B. BHAGAT, in Proceedings of the AIME, Interfaces in Metal–Matrix Composites (March 1986) p. 169.
4. R. B. BHAGAT, *Composites* (1986) 393.
5. *Idem., Mater. Sci. Eng.* **144** (1991) 243.
6. M. A. DELLIS, J. P. KEUSTERMANN and F. DELANNAY, *ibid.* **A135** (1991) 253.

7. Ph VAILLANT, Thesis, University Paris XIII (1993).
8. S. DERMARKAR, *Techniques de l'ingénieur*, Métallurgie, M 250.
9. S. A. GEDEON and I. TANGERINI, *Mater. Sci. Eng.* **A144** (1991) 237.
10. F. A. GIROT, Thesis, University of Bordeaux I (1987).
11. F. A. GIROT, R. FEDOU, J. M. QUENISSET and R. NASLAIN, *J. Reinf. Plas. Comp.* **9** (1990) 456.
12. WANG FENG-GANG, ZHANG-BIN, XU SHI-ZENG, LIU SHU-ZHEN, ZHANG JUN-SHENG, ZHANG YI-GHAO and LU JIAN-SI, in Proceedings of the Eighth International Conference on Composite Materials, Honolulu, July 15–19, 1991, edited by W. Tsai and G. S. Springer (Society for the Advancement of Material and Process, 1991) 18, p. C1.
13. C. COLIN, Y. MARCHAL, F. BOLAND and F. DELANNAY, in Proceedings of EUROMAT 1993, Paris, 8–10 June 1993 (Les éditions de physique) in press.
14. F. DELANNAY, C. COLIN, Y. MARCHAL, L. TAO, F. BOLAND, P. COBZARU, B. LIPS and M. A. DELLIS, in Proceedings of EUROMAT 1993, Paris, 8–10 June 1993 (Les éditions de physique) in press.
15. T. SHINODA, HUA LIU Y. MISHIMA and T. SUZUKI, *Mater. Sci. Eng.* **A146** (1991) 91.
16. A. G. METCALFE, in "Interfaces in Metal Matrix Composite", Composites Materials, Vol 1, edited by A. G. Metcalfe (L. J. Brautman and R. H. Krock Publishers, 1974).
17. A. KELLY and G. J. DAVIES, *Metallurgical Rev.* **10**, no. 37 (1965) 1.
18. S. G. DENNER and R. D. JONES, *Met. Technol.* **4** (1977) 167.
19. S. G. DENNER, R. D. JONES and R. J. THOMAS, *Iron and Steel Inter.* (1975) June, 241–252.
20. V. I. DYBKOV, *J. Mater. Sci.* **25** (1980) 3615.
21. G. EGGELER, Dr. Ing. Thesis, University of Erlangen, (1985).
22. G. EGGELER, W. AUER and H. KAESCHE, *Z. Metallkd.* **77** (1986) 239.
23. *Idem., J. Mater. Sci.* **21** (1986) 3348.
24. E. GEBHARDT and W. OBROWOSKI, *Z. Metallkde.* **44** (1953) 154.
25. G. GÜRTLER and K. SAGEL, *ibid.* **46** (1955) 738.
26. G. GÜRTLER, *Aluminium* **June** (1966).
27. Th. HEUMANN and S. DITTRICH, *Z. Metallkde.* **50** (1959) 617.
28. N. KOMATSU, M. NAKAMURA and H. FUJITA, *J. Jpn. Inst. Light. Met.* **18** (1968) 474.
29. L. N. LARIKOV, V. M. FAL'CHENKO, D. F. POLISHCHUK, V. R. RYABOV and A. V. LOZOVSKAYA, *Prot. Coat. Met.* **3** (1971) 66.
30. D. I. LAYNER and A. K. KURAKIN, *Fiz. Metal. Metalloved* **18** (1964) 148.
31. J. E. NICHOLLS, *Cor. Tech.* **October** (1964) 21.
32. M. NIINOMI and Y. UEDA, *Trans. Jap. Inst. Met.* **23** (1982) 709.
33. Y. UCHIDA, M. FUJITA and Y. HIROSE, *Kinzoku Hyomen Gyutsu* **33** (1982) 537.
34. V. N. YEREMENKO, Ya. V. MATANSON and V. I. DYBKOV, *Avt. Svarka* **2** (1974) 5.
35. *Idem., J. Mater. Sci.* **16** (1981) 1748.
36. R. D. JONES and S. G. DENNER, in Proceedings of the Tenth World Congress in Metal Finishing (Metal Finishing of Japan, Kyoto, 1980).
37. S. RAJAGOPAL, *J. Appl. Met. Work* **1** (1981) 1.
38. A. MORTENSEN, L. J. MASUR, J. A. CORNIE and M. C. FLEMINGS, *Metall. Trans. A* **20A** (1989) 2535.
39. L. J. MASUR, A. MORTENSEN, J. A. CORNIE and M. C. FLEMINGS, *ibid.* **20A** (1989) 2549.
40. V. V. BRAZHKIN, S. V. POPOVA, R. N. VOLOSHIN, L. M. STANEV and I. G. SPIROV, *High Pressure Research* **6** (1992) 333.
41. S. CHATTERJEE, B. MET and A. A. DAS, *Brit. Foundryman* **66** (1973) 118.
42. J. B. CLARK, M. E. THOMAS and P. W. RICHTER, *J. Less-Common Met.* **132** (1987) 181.
43. A. I. KINGON and J. B. CLARK, *High Temp. – High Pres.* **16** (1984) 137.
44. Y. NISHIDA and H. MATSUBARA, *Z. Metallkde.* **71** (1980) 189.
45. J. P. PETITET, L. M. ZHU, M. H. AMBROISE and T. VERDET, in Proceedings of the XXXVIIIth EHPRG Conference, Bordeaux, July 8–13, 1990, edited by G. Demazeau, C. Cross, S. Matar and A. Rahm (High Pressure Research, 1991) p. 7, 22.
46. W. HUME-ROTHERY, in "Elements of structural metallurgy" (The Institute of Metals, Monograph and Report series no. 26, London, 1961).
47. T. SOMA, Y. FUNAYAMA and H. M. KAGAYA, *J. Mater. Sci.* **25** (1990) 3917.
48. M. HANSEN and K. ANDERKO, in "Constitution of binary alloys", edited by J. Elliot (McGraw-Hill, New York, 1958).
49. A. J. BRADLEY and A. TAYLOR, *Proc. Royal. Soc.* **A166** (1938) 353.
50. K. SCHUBERT, "Krystallstrukturen Zweikomponentiger Phasen" (Springer-Verlag, Berlin, 1964).
51. A. GRIGER, A. LENDVAI, V. STEFANIAY and T. TURMEZEY, in "On the phase diagrams of the Al–Fe and Al–Fe–Si systems", Volume 13/14 (Materials Science Forum, Trans. Tech. Publications Ltd., Switzerland, 1987) p. 331.
52. A. GRIGER, V. STEFANIAY, E. KOVACS-CSETENYI and T. TURMEZEY, in Proceedings of the International Workshop, Balatonfüred, Hungary, May, Effect of iron and silicon in aluminium and its alloys (Trans Tech Publications, Switzerland, 1989) p. 17.
53. P. LIU, in "Key engineering materials", edited by I. Kovacs, (1989) pp. 44, 45, 69.
54. Ju. V. NAIDICH, *Prog. Surf. Memb. Sci.* **14** (1981) 448.
55. C. COLIN, Thesis E.N.S.M.P. Paris (1991).
56. J. PHILIBERT, in "Atom movements, diffusion and mass transport in solids" (Les Éditions de Physique, Paris, 1991).
57. V. I. DYBKOV, *J. Mater. Sci.* **21** (1986) 3078.
58. *Idem., ibid.* **21** (1986) 3085.
59. J. SANNIER, J. TROUVE and T. FLAMENT, in "Corrosion des matériaux à haute température" (Les Éditions de Physiques, Paris, 1985).
60. V. G. RIVLIN and G. V. RAYNOR, *Int. Met. Rev.* **3** (1981) 133.
61. D. M. KARPINOS, V. Kh. KADYROV and V. P. MOROZ, *Poroshkovaya Metallurgica* **5** (1974) 63.
62. S. OCHIAI and Y. MURAKAMI, *J. Mater. Sci.* **14** (1979) 831.
63. K. SUGANUMA, *Mater. Lett.* **16** (1993) 22.
64. J. H. WESTBROOK, in "Mechanical properties of intermetallic compounds", Symposium of the Electrochemical Society, 3–7 May (John Wiley, 1959).
65. D. A. BENNETT and D H. KIRKWOOD, *Met. Sci.* **18** (1984) 17.
66. H. W. L. PHILLIPS, *J. Inst. Metal.* **82** (1953–54) 197.
67. V. STEFANIAY, A. GRIGER and T. TURMEZEY, *J. Mater. Sci.* **22** (1987) 539.
68. F. LIHL, E. NACHTIGALL and A. SCHWAIGER, *Z. Metallkde* (1968) 213.
69. P. ROHATGI, R. ASTHANA, *J. O. M.*, **May** (1991) 35.
70. C. N. P. LUPIS, in "Chemical thermodynamics of materials" (North Holland, Amsterdam, 1983).
71 Y. ADDA and M. BEYLELER, in "Physics of solids at high pressure", edited by C. T. Tomizuka and R. M. Emrick (Academic Press, 1965).
72. R. H. DICKERSON, R. F. BONANNO and C. T. TOMIZUKA, in "Physics of solids at high pressure", edited by C. T. Tomizuka and R. M. Emrick (Academic Press, 1965).
73. Y. MURAMATSU, F. ROUX and A. VIGNES, *Trans. J. I. M.* **16** (1975) 61.
74. N. H. NACHTRIEB and C. COSTON, in "Physics of solids at high pressure", edited by C. T. Tomizuka and R. M. Emrick (Academic Press, 1965)

Received 3 February
and accepted 14 November 1994